Hybrid ab initio VB/MM Method − A Valence Bond Ride through Classical Landscapes

Avital Shurki*,† and Hadar A. Crown

Department of Medicinal Chemistry and Natural Products, The Lise Meitner-Minerva Center for Computational Quantum Chemistry, School of Pharmacy, The Hebrew University of Jerusalem, Jerusalem 91120, Israel

Received: August 30, 2005; In Final Form: September 29, 2005

The development of a new hybrid (QM/MM) method, where the QM part is treated by ab initio valence bond (VB) theory is presented. This VB/MM method has the advantages of empirical VB (EVB) methodology but does not rely on empirical parameterization for the quantum part. The method implements embedding of the quantum region of each diabatic state separately, by treating the electrostatic interactions between QM and MM regions classically. Additionally, it assumes that changes of the off diagonal matrix element due to different environments are such that the overall resonance integral does not change. These assumptions are discussed in detail and the validity of the method is shown to be successful in three different bond dissociation processes, where bond dissociation as well as solvation energies compare very well with the experimental data.

Introduction

Most of the chemical reactions in biological systems occur either in solution or in protein molecules. The surroundings (solvent/protein) affect such reactions in a variety of important ways and often determine the relative free energies or stabilities of reactant, transition state, and product molecules. Thus, a prerequisite for a successful study of such reactions are reliable methods that consider the whole environment in the calculation. Current theoretical studies that are trying to incorporate the environment (solvent/protein) effect into calculations of biochemical systems are based on the hybrid quantum mechanical molecular mechanical (QM/MM) approaches.[1−19] These methods treat the reactive fragments quantum mechanically and the rest of the system classically. Several QM/MM approaches have been developed using the combination of semiempirical methods,[2,3,7,8,15,20] ab initio methods,[17−19] or DFT-based methods[21−23] with commonly used force fields.

The theoretical description of the QM part, which accounts for changes in bonding patterns and thus reactivity, has been divided between two major approaches: valence bond (VB) and molecular orbital (MO) theories. While MO-based theory is the dominant computational method, VB theory still remains an important conceptual tool for chemists. VB theory emphasizes electron bond pairs and the VB structures are thus similar to the pictorial resonance structures we usually think of as chemists.[24−26] Furthermore, the VB-configuration mixing (VBCM) model[24−26] enables us to understand in detail the mechanism of barrier formation by following the energies of the VB structures and the resultant mixing of the states along the reaction coordinates. Therefore, VB provides us with better insight into the chemical character of the system and, as such, it has an advantage over MO theory in its ability to deal with problems of chemical reactivity.

Warshel and co-workers[16,27,28] utilized this advantage to develop the empirical valence bond (EVB) method for calculating reactions in solutions and in enzymes. The EVB method obtains the ground-state potential by the mixing of relevant diabatic states, Φ_i, where each state represents a specific bonding and charge configuration. The method considers the diabatic states as independent classical states and thus allows approximation of their energies by MM force fields. The mixing of these diabatic states, determined by the off-diagonal elements of the Hamiltonian, is usually represented by a simple single exponential approximation, which is calibrated by forcing the obtained ground state energy to reproduce the observed activation barrier of the reference reaction (e.g., solution reaction). The EVB potential energy surfaces (PES) focus on the difference between the reactions in different environments (e.g., enzyme and solution), hence the obtained results benefit from the significant reduction of errors and provide an effective way of studying catalysis. Furthermore, since the calibration process necessarily reproduces the correct experimental solution energetics, unrealistic results are prevented. Finally, the EVB holds apparent advantages over MO-based QM/MM methods as far as reactivity problems are concerned. These advantages include the relatively simple description of the reaction coordinate and the similarity of the VB building blocks to the chemist's way of thinking which, in turn, facilitates the interpretation of the results.

These advantages of the EVB approach were appreciated by several researchers, who realized that the reliability of the EVB surfaces depends on its calibration and, in particular, on the estimation of the off diagonal elements, H_{ij}. Various schemes of evaluating H_{ij} utilizing ab initio calculations were developed, such as the Chang and Miller formulation[20,29] or the approximate valence bond (AVB).[30] Other methods, such as the extended EVB[31,32] and multistate EVB (MS-EVB),[33,34] tried to expand upon the EVB method by utilizing several VB forms and ab initio based parameterizations. All these methods may agree with high level ab initio data for the reactants, TS and products geometry, energy, and frequencies, but they do not necessarily

* Corresponding author. E-mail: avital@md.huji.ac.il. Phone: +972-2-675-8696. Fax: +972−2−675−7076.

† Affiliated with the David R. Bloom Center for Pharmacy at the Hebrew University.

10.1021/jp054913x CCC: $30.25
Published on Web 11/17/2005

provide a good description of the global potential energy surface. Truhlar and co-workers presented the multiconfiguration molecular mechanics (MCMM) that uses the Shepard interpolation[35] to obtain the other points on the PES.[36,37]

A different related approach to combine VB and MM is the MMVB method of Bernardi et al.[15,38] The method couples MM force field to a VB Heisenberg Hamiltonian that is parameterized from ab initio CASSCF calculations. Parameterization is currently available only for sp^2 and sp^3 carbon atoms, which limits the treatment to these centers only. Another method is the MOVB/MM method of Mo and Gao.[39,40] This method constructs localized wave functions representing diabatic states from an original MO wave function, and calculates adiabatic PES using configuration interaction. Recently, Shaik, Wu, et al. have developed two distinct VB-based methods for large systems. The first, the VBDFTs, is a Hückel type semiempirical VB method that is parameterized to reproduce DFT energies and applicable to conjugated systems.[41−44] The second method, the VBPCM model, is a VB method that incorporates a polarizable continuum model and thus enables the inclusion of solvent effects within the ab initio VB calculations.

Thus, while some methods either do not capture the whole PES[39,40] or are not designed to study enzymes,[45] most of the available VB-based methods depend on various parameterization schemes.[15,16,20,27−34,36−38,41−44] This need for calibration/parameterization is a major drawback of these methods, which makes them more complex and tedious. Furthermore, the need to parameterize/calibrate the off-diagonal matrix elements makes it difficult to handle more than two diabatic states in one calculation, thereby limiting the type of systems these methods can study. As part of our goal to develop an ab initio VB method that incorporates the environmental effect in its calculations, the present work describes a methodology that couples ab initio VB with MM using concepts taken from the EVB method. This ab initio VB/MM method (referred to as VB/MM hereafter) has all the capabilities and advantages of the EVB approach, while the accuracy of the QM part does not depend on empirical parameterization. The first part of the paper describes the method with the assumptions made and their justification. The method is then applied to several bond dissociation processes as test cases. It is shown that the method is quite successful, both qualitatively and quantitatively.

The VB/MM Theory

Every hybrid QM/MM method requires solving the system's Hamiltonian, which is composed of the quantum part, the classical part, and the coupling between the two parts. We develop here a QM/MM methodology where the QM involves ab initio VB. Here the Hamiltonian of the whole system is written as:

$$H_{\mathrm{VB/MM}} = H^{\mathrm{I}}(\mathrm{VB}) + H^{\mathrm{O}}(\mathrm{MM}) + H^{\mathrm{I,O}}(\mathrm{VB/MM}) \quad (1)$$

where I and O stand for the inner (quantum) and the outer (classical) regions. H^{I}(VB) is the VB Hamiltonian of an isolated quantum region (the gas-phase Hamiltonian) of all the atoms in the inner region, H^{O}(MM) is the energy of all the atoms in the outer region determined by use of an empirical force field, while $H^{\mathrm{I,O}}$(VB/MM) is the Hamiltonian that accounts for all the interactions between the quantum and the classical atoms.

In the VB formalism, the wave function is a linear combination of different VB structures Φ_i:

$$\Psi_{\mathrm{VB}} = \sum_{i}^{N} c_i \Phi_i \quad (2)$$

Thus, solution of the Schrödinger equation using the variational principle leads to a set of linear equations of the form:

$$\sum_{k}^{N} (H_{ik} - \epsilon S_{ik}) c_k = 0 \quad k = 1,2,...N \quad (3)$$

$$H_{ik} = \langle \Phi_i | H | \Phi_k \rangle \quad (4)$$

$$S_{ik} = \langle \Phi_i | \Phi_k \rangle \quad (5)$$

where H_{ij} and S_{ij} are matrix elements of the Hamiltonian and the overlap, respectively. Therefore, when solving the QM/MM Hamiltonian using VB, each one of the matrix elements should be treated separately. Warshel and co-workers utilized this type of treatment in their EVB approach.[16,27,28] Thus, by exploiting the special character of the VB structures being chemically interpretable, the EVB describes each one of the diabatic states together with its environment, using MM. These states are then mixed by an off-diagonal element to give the ground state. Following the work of Warshel and co-workers, we adopted a similar approach; however, the quantum part in our treatment is calculated using ab initio VB.

Current QM/MM methods involve three different coupling schemes.[6] The simplest one represents mechanical embedding of the quantum region, where the electrostatic interactions between the QM and MM regions are calculated classically. A second scheme, which includes the electrostatic interactions between the QM and MM regions by incorporating the classical point charges of the MM region in the core Hamiltonian, allows polarization of the QM region. Finally, the most refined scheme includes also the polarization of the MM region due to the presence of the electric field generated by the QM region.[6]

To achieve adequate accuracy, most ab initio calculations implement the second scheme, i.e., they account for polarization of the QM region. In the case of VB however, implementation of the first scheme, mechanical embedding, in each one of the VB diabatic states separately, should be nearly equivalent to the implementation of the second scheme. Contrary to the MO methodology, here, the charge distribution of each one of the diabatic states translates in a relatively straightforward manner to classical description. Therefore, the specific interactions of each diabatic state with the environment calculated using the classical embedding is also expected to be similar to those calculated using the second scheme. Finally, the mixing of all the diabatic states (each having a different interaction with the environment) is likely to introduce most of the polarization of the QM wave function, due to the environment.

Therefore, the diagonal matrix elements of the Hamiltonian include all the nonbonded interactions calculated classically, as shown below:

$$H_{ii} = H_{ii}^{0}(\mathrm{VB}) + H_{ii}^{\mathrm{int}} \quad (6)$$

where H_{ii}^{0}(VB) is the matrix element of the ith VB structure in an isolated quantum region (the gas-phase matrix element) and H_{ii}^{int} describes the interactions of the quantum diabatic system with the environment. H_{ii}^{int} includes all the nonbonded interactions (such as electrostatic, van der Waals, bulk, etc.). It should

be noted that this formulation relates to the specific case where there are no bonded interactions between the atoms of the QM and the MM regions. The more complicated case where bonded interactions are included is out of the scope of this paper and will be dealt with in future development. H(MM), which is constant for all the different diabatic states and depends only on the configuration of the environment (solvent/protein), is calculated once for each configuration and is added after the eigenvalue problem is solved to all the different H_{ii} matrix elements and to the overall energy.

The next step is evaluation of the off diagonal matrix elements (the resonance integrals) which are not as well established as the diagonal matrix elements, because it is not clear what is the right way to include the interaction between the QM and MM regions. The EVB methodology is based on the assumption that changes in the resonance integral, H_{ij}, due to the environment, are negligible at the crossing point between the states. Thus, for example, the H_{ij} found to calibrate the solution reaction in the EVB calculations is used in turn to describe the same reaction in the protein.[16,27,28] It is important to note that in the EVB scheme where overlap is neglected, H_{ij} represents the reduced resonance integral, β_{ij}, as can be deduced from the definition of the reduced resonance integral:

$$\beta_{ij} = H_{ij} - \frac{1}{2}(H_{ii} + H_{jj})S_{ij}; \quad H_{ii} = H_{jj} \tag{7}$$

Recent VBPCM calculations by Shaik et al.,[45] support this assumption. While looking at their results for the S_N2 reaction, for example, it is seen that changes of the resonance energy, due to incorporation of the solvent effects, are one order of magnitude lower (~3 kcal/mol) compared to the changes in the diabatic energies (~60 kcal/mol). Thus, we apply this approximation by utilizing the same gas-phase reduced resonance integral, β_{ij}, in both solution and protein reactions. Furthermore, we assume that the overlap between the diabatic states is not affected by the environment. These requirements lead to the following expression for H_{ij} at the crossing point of the energy surfaces of the diabatic states:

$$H_{ij} = H_{ij}^0(\mathrm{VB}) + \frac{1}{2}(H_{ii}^{\mathrm{int}} + H_{jj}^{\mathrm{int}})S_{ij}^0 \tag{8}$$

where H_{ij}^0(VB) and S_{ij}^0 are the off-diagonal matrix elements between the ith and jth diabatic states and their relevant overlap in vacuum, respectively. H_{ii}^{int} and H_{jj}^{int} are the interaction energies of the environment with the ith and jth diabatic states, respectively. In the general case, we approximate the off-diagonal matrix element for all points along the curve crossing diagram using the following expression:

$$H_{ij} = H_{ij}^0(\mathrm{VB}) + (w_i H_{ii}^{\mathrm{int}} + w_j H_{jj}^{\mathrm{int}})S_{ij}^0 \tag{9}$$

where w_i and w_j are the respective weights of the ith and jth diabatic states given by the Coulson−Chirgwin formula:[46]

$$w_i = c_i^2 + \sum_{j \neq i}^{N} c_i c_j \langle \Phi_i | \Phi_j \rangle \tag{10}$$

Finally, the eigenvalue problem, as defined in eq 11 with the VB/MM Hamiltonian matrix, $\boldsymbol{H}$, and the vacuum overlap matrix, $\boldsymbol{S}$, is solved, leading to new energies and a new wave function that account for the environment.

$$(\boldsymbol{H} - \epsilon \boldsymbol{S})\boldsymbol{c} = 0 \tag{11}$$

The quality of the results depends largely on the environment, which, in turn, depends largely on the character of the wave function. Thus, the process is repeated iteratively until changes in the wave function due to the environment are small. Moreover, the wave function and in particular the weights of the diabatic states are part of the solution of the eigenvalue problem, which, in turn, is determined by their values. Thus, the process of obtaining the energy is self-consistent and requires an additional iterative route. The overall energy of the system in the solvent/protein, $E_{\mathrm{VB/MM}}$, is given by the following sum:

$$E_{\mathrm{VB/MM}} = \epsilon + E(\mathrm{MM}) \tag{12}$$

where ϵ is the eigenvalue of the VB/MM matrix and E(MM) represents the interaction of all the environment atoms within themselves, calculated by use of empirical force fields (for more details regarding the method see the Appendix).

Computational Methods

Implementation of the method involves coupling between a standard VB package and a molecular mechanics package capable of doing molecular dynamics, which is based on the EVB ideas. In this paper, we use the Xiamen VB (XMVB) package[47,48] for the ab initio quantum calculations and the MOLARIS package[49,50] for all the force field based calculations. An interface program was written to transfer information between the two codes and to calculate the actual VB/MM energy, using the methodology described in the previous section. We studied three different cases of bond dissociation in solution: Li−F, $(CH_3)_3C-Cl$ (t-BuCl), and CH_3–F. Throughout all VB/MM calculations, the solute was treated as the QM portion while the solvent (water molecules) was treated as the MM region of the system.

The isolated quantum region, either individually or as the QM part in the VB/MM calculations of the dissociation curves of the different solutes, was first calculated at different geometries, using the BOVB method.[51,52] In this method, each VB structure has its own set of orbitals. Thus, a minimal set of VB structures was chosen for each system, while the orbitals of each structure were optimized in the presence of the orbitals of the other structures. This procedure leads to a compact wave function which describes both the diabatic as well as the adiabatic states with satisfactory accuracy.[51,52]

The MM part (the water molecules in the classical region) as well as the dynamics utilized the Enzymix force field.[50] The simulation model includes an 18 Å explicit simulation sphere, surrounded by a surface region whose average polarization and radial distribution are determined by the surface-constrained all-atom solvent (SCAAS) model.[53] The surface region is embedded in a bulk continuum region with $\epsilon_w = 80$. Long-range electrostatic effects are treated by the local reaction field (LRF) model.[54]

To obtain suitable configurations of the solvent, equilibration of the system on a proper potential energy surface is required. Thus, based on the EVB approach, each one of the VB structures is defined as a classical state and the potential is expressed as a linear combination of the MM potentials of the different structures with weights taken from the vacuum calculation.

$$V = \sum_{i}^{N} w_i \epsilon_i \tag{13}$$

ϵ_i here is the classical potential energy of the ith diabatic state and N is the overall number of states.

The systems were equilibrated at 300 K for 50 ps, using step size of 1 fs. During the relaxation process, the solute was kept fixed. A single-point VB/MM calculation was then performed on the relaxed configuration and the newly obtained weights served to construct the potential surface for a second relaxation of the environment. Once changes in the diabatic VB/MM weights between two configurations from different relaxations were smaller than 0.05, sampling was carried out for 50 ps, using step size of 1 fs, and 100 different configurations of the environment were collected for each geometry. The free energy was calculated using the potential of mean force (PMF) procedure.[53,55−57] Both the backward and the forward calculations were carried out, and the average of the two is presented.

Applications and Results

The bond dissociation processes of Li−F, t-BuCl and CH_3−F in aqueous solution served as test cases for our VB/MM model. The bond dissociation processes above can be described using the following three VB structures:

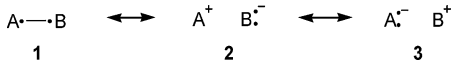

where A−B is the bond to be broken, **1** represents the covalent structure and **2** and **3** represent the two possible ionic structures of that bond. These three systems, which were studied previously by the VBPCM model,[45] represent diverse situations of bond dissociations. On one hand, there are ionic and polar-covalent bonds that undergo homolytic dissociation in the gas-phase yet dissociate into a pair of ions in solution. On the other hand, there are polar-covalent bonds that dissociate to the respective radicals both in vacuum and in the solution. The VB wave function at the dissociation distance in the first case is governed by the covalent structure **1** in the gas phase and one of the ionic structures **2** or **3** in solution, whereas in the second case the wave function is controlled by the covalent structure **1**, both in gas and solution. Thus, during the testing of our VB/MM model, attention was given to its ability to reproduce these behaviors, which indicates, in turn, success of the model in achieving the polarization of the QM wave function due to the environment.

Dissociation of Li−F. LiF was chosen as an example for a typical ionic bond. The quantum calculations utilized the BOVB approach using the 6-31G* basis set. As in the VBPCM calculations,[45] 1S electrons of both the Li and F atoms were frozen at the Hartree−Fock level, thereby leaving eight valence electrons to be explicitly included in the VB calculations. Only two of the above VB structures were included in the calculations of the dissociation process: the covalent and the ionic Li^+ F^-. The contribution of the third structure (the Li^- F^+ ionic configuration) is expected to be negligible, due to its high energy, and thus was not included in the calculations.

Figure 1 displays the weights of the covalent and ionic diabatic structures (marked with dots and plus signs respectively) in the overall wave function both in vacuum (1a) and in solution (1b). It is seen that the model exhibits very clearly the expected qualitative behavior. The wave function of LiF, in the gas phase, is governed by the ionic structure at equilibrium distance and described solely by the covalent contribution at dissociation distance, thus indicating separation into neutral atoms. However, in solution, the model predicts a wave function that is virtually ionic, thus suggesting correctly dissociation of LiF into ion pairs.

This picture is further clarified by looking at the energetic aspects of the model. Figure 2 displays the potential energy curves for the dissociation of LiF in vacuum (1a) and in solution (1b). The individual diabatic (covalent and ionic) profiles are presented in plain lines, while the adiabatic ground-state profile is shown in bold. The overall energy of LiF in solution obtained by the VB/MM procedure includes the classical energy of the environment and thus spans a different energy scale than the system in vacuum. Therefore, the results are presented in kcal/mol relative to the respective dissociation energies of the adiabatic curves, both in the vacuum and in solution. It is seen that the relative energies of the different states in solution changes considerably compared to vacuum. Significant stabilization of both the ionic state and the adiabatic ground state (which are virtually identical) relative to the covalent state is observed in solution. The ground state, for example, is about 245 and 210 kcal/mol more stable than the covalent state at equilibrium distance and long distance, respectively. Assuming that the covalent energy does not change much due to solvation effects, our VB/MM model suggests that the ground-state potential energy curve in aqueous solution is stabilized relative to that in vacuum by approximately 140 and 210 kcal/mol at equilibrium and long distance, respectively. Considering the experimental solvation energies of the separate ions being ca. 115 kcal/mol for Li^+ and ca. 113 kcal/mol for F^-[58], our results, 210 kcal/mol at long distance for the ion pair, are in very good agreement with the experimental data.

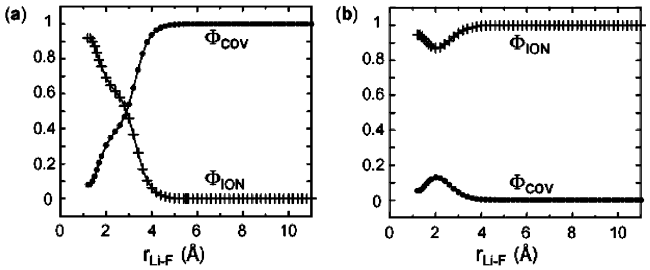

Figure 1. Weights of the VB structures along Li−F dissociation coordinate both in vacuum (a) and in solution (b). The covalent structure (Li•−•F) is marked with dots and the important ionic structure (Li^+ F^-) is marked with plus signs.

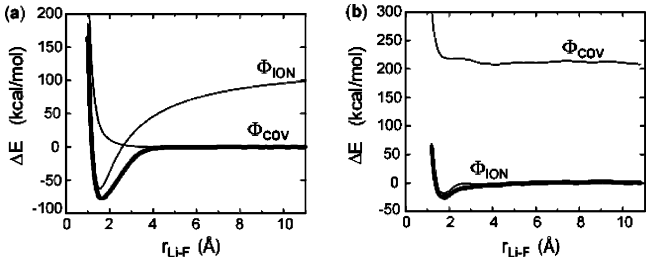

Figure 2. Dissociation energy profile of LiF in vacuum (a) and in solution (b). The diabatic states (both covalent and ionic) are in plain lines, whereas the adiabatic state is shown in bold. Energies are presented relative to the dissociation energy of the adiabatic state in each phase, respectively.

Another interesting energy-related aspect of the results is the dissociation energy of the LiF. The bond energy of LiF in aqueous solution is expected to be less than 5 kcal/mol.[59] The VB/MM model exhibits a dissociation barrier of around 26 kcal/mol. This overestimation of the ion pair bond energy is most likely rooted in the ill-behaved gas-phase energetics. As mentioned by Shaik et al., the crossing between the ionic and the covalent curves in the gas phase occurs earlier (2.6 Å in our calculations) than anticipated (>7 Å) based on considerations of the ionization potential of Li (IP_{Li}), the electron affinity of F (EA_F), and the electrostatic energy of the ionic structure (assuming a flat covalent curve).[45,60] Furthermore, the calculations overestimated the ionic covalent separation energy at long

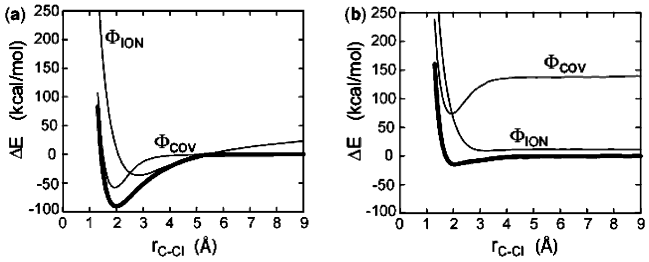

Figure 3. Dissociation energy profile of $(CH_3)_3C-Cl$ in vacuum (a) and in solution (b). The diabatic states (both covalent and ionic) are in plain lines, whereas the adiabatic state is shown in bold. Energies are presented relative to the dissociation energy of the adiabatic state in each phase, respectively.

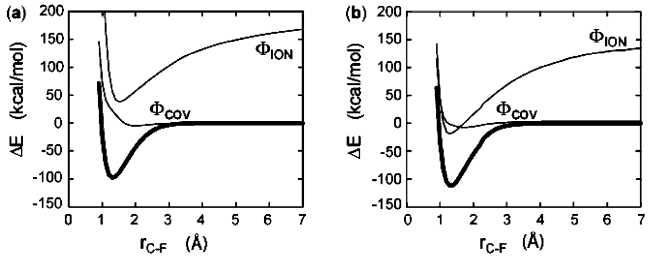

Figure 4. Dissociation energy profile of CH_3-F in vacuum (a) and in solution (b). The diabatic states (both covalent and ionic) are in plain lines, whereas the adiabatic state is shown in bold. Energies are presented relative to the dissociation energy of the adiabatic state in each phase, respectively.

distance to be 100 kcal/mol instead of the expected ca. 45 kcal/mol, based on the same above considerations ($IP_{Li}+EA_F$).[60] These two facts imply that the calculations overestimate bond energy of the ionic curve in the gas phase. This wrong behavior of the gas-phase ionic curve is transferred into the solution ground-state curve, which is dominated by the ionic curve, and thus results with a relatively high dissociation barrier. A better description of the gas-phase curves would result with a smaller dissociation barrier for the ion pair.

Another aspect of the solvent effect concerns the geometry of LiF. The VB/MM model predicts that the equilibrium bond length shifts from 1.6 Å in the gas phase to 1.8 Å in water, in accordance with the expected behavior. Finally, the results obtained here are in good agreement with the results obtained with the VBPCM model and display somewhat better quantitative behavior when compared with the experimental data.

Dissociation of t−BuCl. The second example is the dissociation of the C−Cl bond in tertiary-butyl chloride (t-BuCl), a polar-covalent bond that is expected to behave differently in vacuum and in solution. The calculations employed the BOVB approach for the calculation of the solute using the 6-31G basis set. All the core and π-electrons were frozen at the HF level, thereby, leaving six pairs of electrons to be calculated explicitly at the BOVB level. The VB structure that involves a carbanion and a positive halogen was left out of the calculation.

Figure 3 presents the t-BuCl dissociation potential-energy profiles of the different diabatic (plain lines) as well as the adiabatic (bold line) states both in vacuum 3a and in solution 3b. It is evident that the covalent curve dominates the ground state at long distance in vacuum, thereby suggesting dissociation into radicals. In solution, on the other hand, the ground state is ruled by the ionic state, thus indicating dissociation into ions, in accordance with the first step of the S_N1 mechanism, which is characteristic of t-BuCl. Furthermore, by disregarding changes in the covalent state due to solvation, as assumed before, it is seen that in solution the ground state is stabilized relative to that in vacuum by about 45 kcal/mol at equilibrium and 140 kcal/mol at long distance. It is also seen that the stabilization comes mainly from the stabilization of the ionic state that stabilizes ca. 67 kcal/mol at equilibrium distance and ca. 167 kcal/mol at long distance.

Finally, the calculated vacuum dissociation energy amounts to 91 kcal/mol and compares favorably with the expected 80 kcal/mol.[61,62] This bond energy exhibits considerable reduction in solution, turning into a calculated value of 14.5 kcal/mol, which is in good agreement with the expected 19.5 kcal/mol.[63] Yet, as in the VBPCM model,[45] the VB/MM model was not successful in describing the ion-pair intermediate.[64−66] In the VBPCM analysis of the C−Cl bond in t-BuCl in vacuum (based on calculations at the VBSCF level),[45] the double crossing of the ionic and covalent curves was suggested to be an artifact of an erroneous description of the ionic state whose stabilization is overvalued in vacuum calculations leading to the underestimation of the gap between the covalent and ionic structures at long distance. This behavior recurs at the BOVB level, where the ionic covalent gap is calculated to be 27 kcal/mol at 10 Å instead of the estimated experimental value of ca. ∼84 kcal/mol (based on ionization potential and electron affinity considerations).[45] Therefore, the low dissociation barrier and the absence of an ion-pair intermediate in solution could be a result of underestimation of the ionic dissociation barrier in vacuum, and a better vacuum description should lead to better results.

Dissociation of CH_3-F. The first two examples demonstrate that the model clearly favors ionic states while they are expected to be stable in solution. Thus, to verify that it does not convert every gas-phase picture into a situation where the ionic structure becomes more stable than the covalent state, our last example was chosen to be the dissociation of the C−F bond in CH_3F. Here, the molecule is expected to undergo a homolytic dissociation, thus resulting in neutral fragments, both in the gas phase and in solution. The quantum calculations utilized the BOVB approach and, again, due to expected negligence of the contribution of the structure that involves a carbanion and a positive halogen, only two of the three VB structures ($H_3C\bullet-\bullet F$ and $H_3C^+\ F^-$) were included in the calculations. Four inner electrons of the C and F atoms were frozen at the HF level, while the remaining 14 electrons were explicitly calculated. The VB calculations employed the 6-31G* basis set.

Figure 4 displays the potential energy curves for the dissociation of CH_3F, both in vacuum (4a) and in solution (4b). As expected, the covalent structure dominates the ground-state curve at long distance, both in the gas phase and in solution, suggesting homolytic dissociation in both cases. The equilibrium distance, on the other hand, has similar contributions of both states leading, as mentioned by Shaik et al., to bond energy which originates to a great extent from the resonance energy between the ionic and the covalent states.[45] Furthermore, from the adiabatic potential we can deduct that the solvent does not affect the molecule's geometry, leading to an equilibrium bond length of 1.3 Å in both phases.

Again, assuming that the covalent state has not changed much relative to the gas phase, it is obvious that the ionic structure has stabilized. The relative stabilization of the ionic structure in solution is about 50 kcal/mol at equilibrium geometry and is reduced at longer C−F distances approaching ∼40 kcal/mol at 7 Å. Both diabatic states (covalent and ionic) presented in the figure are fully optimized in vacuum. Generally, one would expect a much greater stabilization of the ionic structure, especially at long distances. Here, as pointed out by Shaik et al.,[45] the energy gap between the ionic and the covalent states

should virtually fade away in solution since the stabilization of the methyl cation and the fluorine anion, due to solvation, is expected to be of the same order as the sum of the ionization potential and the electron affinity of the respective radicals (149 kcal/mol). This value represents in both cases the above energy gap between the two states in vacuum, and therefore it is expected that the two quantities will cancel each other out. Thus, our predicted stabilization of about 40 kcal/mol for the ionic structure, which reduces the ionic−covalent energy gap from ∼170 kcal/mol in vacuum to ∼130 kcal/mol in solution is largely underestimated.

Furthermore, contrary to our results, the stabilization of the ionic state in solution is expected to increase rather than decrease when the C−F distance increases. This behavior of the ionic structure can originate from several factors. First, as can be seen from the figure, the gap between the ionic and the covalent states at long distance is already too large in vacuum (ca. 170 instead of the expected 149 kcal/mol). A choice of a better basis set may therefore improve the results both in vacuum and in solution. A second cause for the ionic behavior can be an incomplete treatment of the solvent. The expected disappearance of the gap between the two diabatic states is based on considerations that are related to pure states (solvation of the respective separate ions versus ionization potential and electron affinity of the respective radicals). However, while both diabatic states are fully optimized in vacuum, the description of the ionic state in solution is deficient. The calculations involved solvent configurations which were equilibrated to describe correctly the ground adiabatic state. These configurations served also for the calculation of the individual ionic and covalent diabatic states. However, the ground state at equilibrium distance is described by an almost equal contribution of both the ionic and the covalent structures, and at long distance the state is defined by the covalent structure only. Therefore, these solvent configurations that are adjusted to best describe the adiabatic ground state are inappropriate for the description of the ionic structure, leading to its inadequate stabilization. Furthermore, in tune with the wave function of the adiabatic state, the organization of the solvent molecules around the solute is fairly random at long distance while it undergoes partial polarization at equilibrium distance. This explains why the stabilization of the ionic structure is worst at long distance. A proper calculation should have included independent relaxation of the environment for each one of the diabatic states separately. In fact, using ab initio terminology, the effect we encounter here can be referred to as a consequence of using a mean field approximation for the environment. Thus, similar to the inclusion of the dynamic correlation in the BOVB approach,[67,68] which overcomes the mean field problem, here too adjustment of the environment to each one of the diabatic states independently should result with a better description. Finally, insufficient solvent sampling may also contribute to the underestimation of the stabilization of the ionic state at long distance.

Conclusions

This work presented a hybrid method that combines ab initio VB with MM using ideas taken from the EVB approach. In addition, the method maintains all the advantages of the EVB methodology. It can be used in a comparative manner, thus, helping to reduce mistakes. It uses force fields for the interactions with the environment, thereby, leading to reliable results. It also gives a clear and simple picture of reactivity. Furthermore, the VB/MM method overcomes some of the disadvantages of the EVB approach by allowing calculations of as many VB structures as one wishes with no special effect. Consequently, the method provides the exact wave function without the need to guess it. Additionally, it is not essential to parameterize the quantum region since the QM part in the VB/MM method is calculated with ab initio methods.

The method was tested on three different bond dissociation processes in solution and was found valid. The results obtained are usually in good agreement with the experimental data. Differences from the experiment were shown to originate from two main causes. The first is a poor representation of the system in the gas phase − a problem that can be dealt with by providing a better gas-phase description (different level of calculation such as the VBCI[69] or higher basis sets). The second source of discrepancy is the mean field approximation employed here for calculation of each one of the separate VB states; an approximation that can be overcome by calculating each state in its own equilibrated environment. It is shown that, similar to the VBPCM method, the VB/MM can supply the VB wave function of the system. The accuracy of the VB/MM method depends on configuration sampling of the environment and as such its computational cost is greater than the VBPCM. Yet, an important advantage of the VB/MM is its ability to calculate any system that can be described with force fields, thus, it is not limited to solvents. Therefore, future applications of the method in biological systems will benefit from its advantages and lead to stimulating insights.

Acknowledgment. The authors thank Dr. Marek Štrajbl for enlightening discussions and suggestions. For financial support, we thank the Alex Grass Center for Drug Design and Synthesis of Novel Therapeutics, the David R. Bloom Center for Pharmacy at the Hebrew University, the Stephanie Gross Foundation, and the Dreikurs Research Fund.

Appendix

A detailed explanation of the VB/MM method is given below. To clarify the explanation, a detailed procedure will be exemplified on a two-state system, but it should be noted that any number of states can be considered in the calculation. The details of the procedure for a specific geometry of the inner-part atoms are outlined below:

1. The first step involves an ab initio VB calculation of the system in vacuum at any level of interest and results in the gas-phase energetics (H^0_{11}, H^0_{22}, and H^0_{12}), as well as the wave function, the respective diabatic weights w_1 and w_2, and the overlap, S^0_{12}.

2. The environment of the system is relaxed to a state described by the wave function, obtained in the previous step. This step utilizes the EVB methodology that enables relaxation of the system to any chosen wave function.

3. Using a relaxed configuration of the environment, the two-state VB/MM Hamiltonian matrix is defined as follows:

$$\boldsymbol{H} = \begin{pmatrix} H^0_{11}(\mathrm{VB}) + H^{\mathrm{int}}_{11} & H^0_{12}(\mathrm{VB}) + (w_1{}^{(i-1)}H^{\mathrm{int}}_{11} + w_2{}^{(i-1)}H^{\mathrm{int}}_{22})S^0_{12} \\ H^0_{12}(\mathrm{VB}) + (w_1{}^{(i-1)}H^{\mathrm{int}}_{11} + w_2{}^{(i-1)}H^{\mathrm{int}}_{22})S^0_{12} & H^0_{22}(\mathrm{VB}) + H^{\mathrm{int}}_{22} \end{pmatrix} \tag{14}$$

where $w_1^{(i-1)}$ and $w_2^{(i-1)}$ stand for the weights from the previous iteration (such as the gas-phase weights) acting as a guess in the first iteration.

4. The eigenvalue problem, as defined in eq 15 with the above Hamiltonian matrix (eq 14) and the vacuum overlap matrix, is solved resulting in new energies, wave function and weights $w_1^{(i)}$ and $w_2^{(i)}$.

$$(\boldsymbol{H} - \epsilon \boldsymbol{S})\boldsymbol{c} = 0 \tag{15}$$

5. Steps 3 and 4 are repeated until the energy difference between two iterations reaches a given threshold, which was set for this study at 0.1 kcal/mol.

6. Steps 2 to 5 are repeated until the difference in weights of the diabatic states between two repeats reaches a given threshold, which was set for this study at 0.05. It should be noted that this last step is essential to ensure correct sampling of the environment configurations.

7. Finally, the overall energy, $E_{\mathrm{VB/MM}}$, is given by the sum of the eigenvalue, ϵ, obtained above and the energy of the environment:

$$E_{\mathrm{VB/MM}} = \epsilon + E(\mathrm{MM}) \tag{16}$$

References and Notes

(1) Warshel, A.; Levitt, M. *J. Mol. Biol.* **1976**, *103*, 227.
(2) Warshel, A. *Annu. Rev. Biophys. Biomol. Struct.* **2003**, *32*, 425.
(3) Field, M. J.; Bash, P. A.; Karplus, M. *J. Comput. Chem.* **1990**, *11*, 700.
(4) Field, M. *J. Comput. Chem.* **2002**, *23*, 48.
(5) Cui, Q.; Elstner, M.; Kaxiras, E.; Frauenheim, T.; Karplus, M. *J. Phys. Chem. B* **2001**, *105*, 569.
(6) Bakowies, D., Thiel, W. *J. Phys. Chem.* **1996**, *100*, 10580.
(7) Friesner, R. A.; Beachy, M. D. *Curr. Opin. Struct. Biol.* **1998**, *8*, 257.
(8) Monard, G.; Merz, K. M., Jr. *Acc. Chem. Res.* **1999**, *32*, 904.
(9) Gao, J. *Reviews in Computational Chemistry*; VCH: New York, 1995; Vol. 7.
(10) Vasilyev, V. V.; Bliznyuk, A. A.; Voityuk, A. A. *Int. J. Quantum Chem.* **1992**, *44*, 897.
(11) Théry, V.; Rinaldi, D.; Rivail, J.-L.; Maigret, B.; Ferenczy, G. G. *J. Comput. Chem.* **1994**, *15*, 269.
(12) Thompson, M. A.; Glendening, E. D.; Feller, D. *J. Phys. Chem.* **1994**, *98*, 10465.
(13) Thompson, M. A.; Schenter, G. K. *J. Phys. Chem.* **1995**, *99*, 6374.
(14) Murphy, R. B.; Philipp, D. M.; Friesner, R. A. *J. Comput. Chem.* **2000**, *21*, 1442.
(15) Bernardi, F.; Olivucci, M.; Robb, M. A. *J. Am. Chem. Soc.* **1992**, *114*, 1606.
(16) Åqvist, J.; Warshel, A. *Chem. Rev.* **1993**, *93*, 2523.
(17) Singh, U. C.; Kollman, P. A. *J. Comput. Chem.* **1986**, *7*, 718.
(18) Štrajbl, M.; Hong, G.; Warshel, A. *J. Phys. Chem. B* **2002**, *106*, 13333.
(19) Stanton, R. V.; Hartsough, D. S.; Merz, K. M., Jr. *J. Comput. Chem.* **1995**, *16*, 113.
(20) Chang, Y.-T.; Miller, W. H. *J. Phys. Chem.* **1990**, *94*, 5884.
(21) Wesolowski, T. A.; Warshel, A. *J. Phys. Chem.* **1993**, *97*, 8050.
(22) Hong, G.; Štrajbl, M.; Wesolowski, T. A.; Warshel, A. *J. Comput. Chem.* **2000**, *21*, 1554.
(23) Olsson, M. H. M.; Hong, G.; Warshel, A. *J. Am. Chem. Soc.* **2003**, *125*, 5025.
(24) Shaik, S. S. A Qualitative Valence Bond Approach to Organic Reactions. In *New Theoretical Concepts for Understanding Organic Reactions NATO ASISeries*; Bertran, J., Csizmadia, G. I., Eds.; Kluwer: Dordrecht, Holland, 1989; Vol. C267.
(25) Shaik, S. S.; Hiberty, P. C. Curve Crossing Diagrams as General Models for Chemical Reactivity and Structure. In *Theoretical Concepts for Chemical Bonding*; Maksic, Z. B., Ed.; Springer-Verlag: Berlin, 1991; Vol. 4; p 324.
(26) Shaik, S.; Shurki, A. *Angew. Chem., Int. Ed. Engl.* **1999**, *38*, 586.
(27) Warshel, A.; Weiss, R. M. *J. Am. Chem. Soc.* **1980**, *102*, 6218.
(28) Warshel, A. *Computer Modeling of Chemical Reactions in Enzymes and Solutions*; John Wiley & Sons: New York, 1991.
(29) Chang, Y.-T.; Minichino, C.; Miller, W. H. *J. Chem. Phys.* **1992**, *96*, 4341.
(30) Grochowski, P.; Lesyng, B.; Bala, P.; McCammon, J. A. *Int. J. Quantum Chem.* **1996**, *60*, 1143.
(31) Vuilleumier, R.; Borgis, D. *J. Mol. Struct.* **1997**, *436*−*437*, 555.
(32) Vuilleumier, R.; Borgis, D. *Chem. Phys. Lett.* **1998**, *284*, 71.
(33) Schmitt, U. W.; Voth, G. A. *J. Phys. Chem. B* **1998**, *102*, 5547.
(34) Schmitt, U. W.; Voth, G. A. *J. Chem. Phys.* **1999**, *111*, 9361.
(35) Ischtwan, J.; Collins, M. A. *J. Chem. Phys.* **1994**, *100*, 8080.
(36) Kim, Y.; Corchado, J. C.; Villà, J.; Xing, J.; Truhlar, D. G. *J. Chem. Phys.* **2000**, *112*, 2718.
(37) Albu, T. V.; Corchado, J. C.; Truhlar, D. G. *J. Phys. Chem. A* **2001**, *105*, 8465.
(38) Garavelli, M.; Ruggeri, F.; Ogliaro, F.; Bearpark, M. J.; Bernardi, F.; Olivucci, M.; Robb, M. A. *J. Comput. Chem.* **2003**, *24*, 1357.
(39) Mo, Y. R.; Gao, J. L. *J. Phys. Chem. A* **2000**, *104*, 3012.
(40) Mo, Y. R.; Gao, J. L. *J. Comput. Chem.* **2000**, *21*, 1458.
(41) Wu, W.; Zhong, S. J.; Shaik, S. *Chem. Phys. Lett.* **1998**, *292*, 7.
(42) Wu, W.; Shaik, S. *Chem. Phys. Lett.* **1999**, *301*, 37.
(43) Wu, W.; Danovich, D.; Shurki, A.; Shaik, S. *J. Phys. Chem. A* **2000**, *104*, 8744.
(44) Wu, W.; Luo, Y.; Song, L. C.; Shaik, S. *Phys. Chem. Chem. Phys.* **2001**, *3*, 5459.
(45) Song, L. C.; Wu, W.; Zhang, Q.; Shaik, S. *J. Phys. Chem. A* **2004**, *108*, 6017.
(46) Chirgwin, H. B.; Coulson, C. A. *Proc. R. Soc. London Ser. A* **1950**, *2*, 196.
(47) Song, L. C.; Wu, W.; Mo, Y.; Zhang, Q. XMVB-0.1 − An ab initio Non-Orthogonal Valence Bond Program; Xiamen University, Xiamen 361005, China, 2003.
(48) Wu, W.; Mo, Y.; Cao, Z.; Zhang, Q. A Spin Free Approach for Valence Bond Theory and Its Application. In *Valence Bond Theory*; Cooper, D. L., Ed.; Elsevier: Amsterdam, 2002; p 143.
(49) Chu, Z. T.; Villa, J.; Štrajbl, M.; Schutz, C. N.; Shurki, A.; Warshel, A. MOLARIS version beta9.05; University of Southern California, Los-Angeles, 2004; in preparation.
(50) Lee, F. S.; Chu, Z. T.; Warshel, A. *J. Comput. Chem.* **1993**, *14*, 161.
(51) Hiberty, P. C.; Flament, J. P.; Noizet, E. *Chem. Phys. Lett.* **1992**, *189*, 259.
(52) Hiberty, P. C.; Shaik, S. Breathing-Orbital Valence Bond − A Valence Bond Method Incorporating Static and Dynamic Electron Correlation Effects. In *Valence Bond Theory*; Cooper, D. L., Ed.; Elsevier: Amsterdam, 2002; p 187.
(53) King, G.; Warshel, A. *J. Chem. Phys.* **1990**, *93*, 8682.
(54) Lee, F. S.; Warshel, A. *J. Chem. Phys.* **1992**, *97*, 3100.
(55) Burkert, U.; Allinger, N. L. *Molecular Mechanics*; American Chemical Society: Washington D. C., 1982.
(56) Roux, B. *Comput. Phys. Commun.* **1995**, *91*, 275.
(57) Muller, R. P.; Warshel, A. *J. Phys. Chem.* **1995**, *99*, 17516.
(58) Marcus, Y. *Ion Solvation*; John Wiley and Sons Ltd: Chichester, 1985.
(59) Karim, O. A.; McCammon, J. A. *J. Am. Chem. Soc.* **1986**, *108*, 1762.
(60) Kauzmann, W. In *Quantum Chemistry*; Academic Press: New York, 1957; p 536.
(61) Sanderson, R. T. *Polar Covalence*; Academic: New York, 1983.
(62) Sanderson, R. T. *Chemical Bonds and Bond Energy*; Academic: New York, 1976.
(63) Jorgensen, W. L.; Buckner, J. K.; Huston, S. E.; Rossky, P. J. *J. Am. Chem. Soc.* **1987**, *109*, 1891.
(64) Lowry, T. H.; Richardson, K. S. *Mechanism and Theory in Organic Chemistry*, 3rd ed.; Harper & Row: Cambridge, 1995.
(65) Kim, H. J.; Hynes, J. T. *J. Am. Chem. Soc.* **1992**, *114*, 10508.
(66) Hartsough, D. S.; Merz, K. M., Jr. *J. Phys. Chem.* **1995**, *99*, 384.
(67) Hiberty, P. C.; Shaik, S. *Theor. Chem. Acc.* **2002**, *108*, 255.
(68) Song, L. C.; Wu, W.; Dong, K.; Hiberty, P. C.; Shaik, S. *J. Phys. Chem. A* **2002**, *106*, 11361.
(69) Wu, W.; Song, L. C.; Cao, Z.; Zhang, Q.; Shaik, S. *J. Phys. Chem. A* **2002**, *106*, 2721.